Amino Acids
https://doi.org/10.1007/s00726-023-03249-6

ORIGINAL RESEARCH PAPER

Phenolic compounds as histone deacetylase inhibitors: binding propensity and interaction insights from molecular docking and dynamics simulations

Abdullahi Ibrahim Uba[1] · **Gokhan Zengin**[2]

Received: 26 December 2022 / Accepted: 6 February 2023

Abstract
Histone deacetylases are well-established target enzymes involved in the pathology of different diseases including cancer and neurodegenerative disorders. The approved HDAC inhibitor drugs are associated with cellular toxicities. Different phenolic compounds have been shown to possess inhibitory activities against HDACs and are, therefore, considered safer alternatives to synthetic compounds. Here, we elucidated the binding mode and calculated the binding propensity of some of the top phenolic compounds against different isoforms representing different classes of Zn^{2+} ion-containing HDACs using the molecular docking approach. Our data reaffirmed the activity of the studied phenolic compounds against HDACs. Binding interaction analysis suggested that these compounds can block the activity of HDACs with or without binding to the active site zinc metal ion. Furthermore, molecular dynamics (MD) simulations were carried out on the selected crystal and docking complexes of each selected HDAC isoform. Analysis of root-mean-square displacement (RMSD) showed that the phenolic compounds demonstrated a stable binding mode over 50 ns in a way that is comparable to the cocrystal ligands. Together, these findings can aid future efforts in the search for natural inhibitors of HDACs.

Keywords HDACs · Phenolic compounds · Molecular docking · Zn^{2+} ion binding

Introduction

Histone deacetylase enzymes catalyze the removal of an acetyl group from an ε-N-acetyl lysine amino acid on a histone. This allows the DNA to wrap around the histone tightly to prevent gene expression. HDACs are grouped into four classes based on phylogenetic analyses and sequence homologies with the yeast proteins. Class I HDACs (1, 2, 3 and 8) share sequence homology with yeast Rpd3, Hos1, and Hos2. Class IIa HDACs (4, 5, 7 and 9) and Class IIb (HDACs 6 and 10) share similar sequences with yeast HDA1 and Hos3. Class III are sirtuins (1–7), and class IV HDAC11. Classes I, II, and IV are zinc-dependent, whereas class III members are nicotinamide adenine dinucleotide (NAD)-containing enzymes (Milazzo et al. 2020). Therefore, this study focuses on classes I, II, and IV.

Class I HDACs are homologous to the yeast HDAC Rpd3 and harbor a more conserved deacetylase domain compared with other classes, are ubiquitously expressed, and are predominantly located in the nucleus, where they act on histones (Watson et al. 2012). Class I HDACs also act as catalytic subunits with corepressor complexes to repress gene expression. For example, HDACs 1 and 2 form a complex with the nucleosome remodeling and deacetylase complex (NuRD) (Bornelöv et al. 2018), transcriptional regulatory protein Sin3A (Saunders et al. 2017), a corepressor of REST (CoREST) (You et al. 2001), and the mitotic deacetylase complex (MiDAC) (Milazzo et al. 2020). HDAC3 is recruited to the SMRT/N-CoR corepressor complex (Guenther et al. 2001). However, HDAC8 functions alone without forming a large complex (Hu et al. 2000).

Class II HDACs share high sequence similarity with yeast HDA1, with a conserved deacetylase domain at their

Handling editor: Sébastien Albrecht.

✉ Abdullahi Ibrahim Uba
abdullahi.iu2@gmail.com

✉ Gokhan Zengin
gokhanzengin@selcuk.edu.tr

[1] Department of Molecular Biology and Genetics, Istanbul AREL University, 34537 Istanbul, Turkey

[2] Department of Biology, Science Faculty, Selcuk University, 42130 Konya, Turkey

Published online: 12 February 2023

C-terminus. Class IIa HDACs (HDAC4, 5, 7 and 9) harbor a unique adapter domain in the N-terminus which serves as a docking site of the DNA-binding transcription factor MEF2 (Muslin 2000). Class IIa HDACs have also been shown to interact with the SMRT/N-CoR-HDAC3 complex (Hudson et al. 2015). The highly conserved active site tyrosine residue in class I HDACs is replaced with histidine in class IIa HDACs. Consequently, class IIa demonstrates lower enzymatic activity compared with class I HDACs. The catalytic domains of class II HDACs harbor another zinc ion-binding site referred to as the structural zinc ion-binding subdomain. Many of the class IIa-specific residues are found in this structural zinc ion-binding site and at the entry site to the catalytic site (Park and Kim 2020). Class IIb HDACs (HDAC6 and 10) have a characteristic extension (tail domain) at the C-terminus. HDAC6 contains two deacetylase domains (CD1 and CD2) and a C-terminal zinc finger ubiquitin-binding domain (Zhang et al. 2006). HDAC10 has only one deacetylase domain and a leucine-rich repeat domain at its C-terminus (Hai et al. 2017). Both HDACs 6 and HDAC10 are typically found in the cytoplasm. HDAC6 acts on nonhistone proteins to regulate important cellular processes. For example, HDAC6 deacetylates α-tubulin to control the microtubule dynamics; acts on chaperones, cortactin, and IFNαR; and plays regulatory roles in autophagy as well as hepatic metabolism (Li et al. 2012). Class IV only member HDAC11, is predominantly expressed in the brain, heart, kidneys, testis, and skeletal muscles, and is localized in the nucleus (Gao et al. 2002). HDAC11 shares structural similarities with both classes I and II HDACs, harboring a catalytic domain containing 268 amino acid residues. HDAC11 is a multifaceted enzyme with a very efficient long-chain fatty acid deacylase activity. This isoform has been shown to have preference for removing long-acyl rather than acetyl groups (Moreno-Yruela et al. 2018).

HDACs play vital roles in the cell and disruption of their normal functions leads to different cellular pathogenesis including cancers and neurodegenerative diseases (Shukla and Tekwani 2020; Volmar and Wahlestedt 2015; Simões-Pires et al. 2013). For instance, overexpression of both classes I and II HDACs in a variety of cancers has been comprehensively reviewed (Wang et al. 2020; Alseksek et al. 2022; Pant et al. 2020; Li and Seto 2016). So far, most clinically effective HDAC inhibitors have demonstrated good outcomes against hematological neoplasms (T-cell lymphomas and multiple myeloma (MM)). To date, 5 HDAC inhibitors have been approved by the FDA for the treatment of cancers: vorinostat, belinostat, romidepsin, tucidinostat, and panobinostat. Details about their structures (hydroxamic acid and nonhydroxamic acid) and efficacy on specific cancer types have been comprehensively reviewed by Bondarev et al. (2021). These drugs are nonselective and thus show adverse effects. In search of potential selective molecular scaffolds that could be further optimized, several computer-aided drug design approaches were successfully applied, including structure-based (Uba and YelekÇİ 2017; Ibrahim Uba and Yelekçi 2019; Uba and Yelekçi 2017, 2018a) and ligand-based virtual screenings (Uba and Yelekçi 2018b). Also, several compounds of natural origin have demonstrated HDAC inhibition properties. For example, trichostatin A (TSA), originally extracted from *Streptomyces hygroscopicus,* possesses potent HDAC inhibitory activity. TSA can trigger cell differentiation and induces cell cycle arrest in both normal and cancer cells together via HDAC inhibition (Tsuji et al. 1976). Other examples of HDAC inhibitors from natural sources include spiruchostatin A, largazole, burkholdac A, lycorine, and many more (Losson et al. 2016). Moreover, phenolic compounds such as caffeic acid, p-coumaric acid, and ferulic acid have been shown to protect the heart via HDAC inhibition (Roy and Stanely Mainzen Prince 2013; Panda et al. 2016; Wang et al. 2013). In another study, a series of phenolic compounds including quercetin, kaempferol, luteolin, and chlorogenic acid were reported to show strong activity against HDAC8 (Shimizu and Mira 2015). Also, a computational study showed the binding propensity of apigenin and luteolin against class I HDAC isoforms and concluded that these compounds may replace synthetic HDAC inhibitors for cancer treatment (Ganai et al. 2018). Recently, molecular docking was used to demonstrate the binding of flavones (flavone, apigenin, and luteolin) to HDACs 1 and 2. Interestingly, findings from the study cited above showed that these compounds mimic the binding of an existing HDAC inhibitor vorinostat (Scafuri et al. 2020). Here, to gain more insights into their binding behavior, more phenolic compounds were docked into the active sites of some selected HDACs representing each class of zinc ion-containing HDACs and molecular dynamics simulations were carried out to examine the stability of their binding mode over time.

Materials and methods

Protein preparation

The following crystal structures of selected HDAC isoforms complexed with different ligands were retrieved from the protein data bank (PDB) (https://www.rcsb.org/): HDAC1 (PDB ID: 5ICN) (Watson et al. 2016), HDAC8 (PDB ID: 5FCW) (Tabackman et al. 2016), HDAC4 (PDB ID: 2VQQ) (Bottomley et al. 2008), HDAC6 (PDB ID: 5EDU) (Hai and Christianson 2016). In the absence of the crystal structure of human HDAC10, the homology-modeled structure built previously by our group (Ibrahim Uba and Yelekçi 2019) was also retrieved. Water molecules and non-interacting ions were removed. The binding coordinates of each inhibitor in

the respective protein structure were recorded before removing the cocrystal ligands. To prepare the protein structures for molecular docking, the pKa of titratable residues in each protein was predicted using the "Playmolecule ProteinPrepare" module (Martínez-Rosell et al. 2017) and was then used to prepare the proteins at physiological pH of 7.4.

The 3D structures of selected ligands were downloaded from the PubChem database (https://pubchem.ncbi.nlm.nih.gov/) and their geometry was optimized using Frog2 (Miteva et al. 2010).

Molecular docking

A series of phenolic compounds were docked into the active sites of selected HDAC isoforms. In addition**,** each cocrystal ligand was redocked into its cognate protein to validate AutoDock's binding pose prediction accuracy. The docking input grid file was prepared using AutoDockTools 1.5.6, followed by docking using AutoDock 4.2.6 (https://autodock.scripts.edu) (Morris et al. 2009). During the process, the energy grid box of dimensions 55, 55, and 55 Å for HDACs 1, 4, and 8; 65, 65, 65 Å for HDAC6, and 60, 60, 60 Å for HDAC10. These parameters were chosen according to the size of the binding pocket of each isoform. The Lamarckian genetic algorithm was used for ligand conformational search. For each compound, 20 independent runs were performed, and the distinct ligand conformers were generated and docked randomly into the binding pocket of these enzymes. The program randomly assigned torsion angles to rotatable bonds, and energy valuation was set to 20,000,000. The binding energy of each ligand pose was calculated, and protein–ligand interactions were visualized using Biovia Discovery Studio Visualizer 4.5.

Molecular dynamics simulation

To examine the stability of ligand-binding mode, molecular dynamics (MD) simulations were carried out on the following complexes: crystal structure of HDAC1 complexed with a novel peptide inhibitor (PDB ID: 5ICN), docking complex of HDAC1 with rutin; crystal structure of HDAC8 in complex with hydroxamic acid-based inhibitor (PDB ID: 5FCW), docking complex of HDAC8 with quercetin; crystal structure of HDAC4 in complex with trifluoromethylketone inhibitor (PDB ID: 2VQQ), docking complex of HDAC4 with chlorogenic acid, crystal structure of HDAC6 in complex with trichostatin A (PDB ID: 5EDU), docking complex of HDAC6 with chlorogenic acid; unbound homology-modeled structure of HDAC10, and its docking complex with gallic acid were generated using the CHARMM-GUI server, employing the CHARMM36 force field (http://www.charmm-gui.org/) (Lee et al. 2015). Ligands were parameterized using the CHARMM General Force Field (CGenFF) (https://cgenff.paramchem.org/). All the systems were solvated using the TIP3 water model and neutralized with NaCl to the ionic concentration of 0.2 M. All simulations were carried out using NAMD software (Phillips et al. 2005). The energy of each system was minimized for 50 ps by the steepest descent method and then equilibrated for 5 ns in standard number of particles, volume, temperature (NVT) ensemble. Finally, 50 ns-long production MD simulation runs were performed in standard number of particles, pressure, temperature (NPT) ensemble on each system. During the production run, the time step and collection interval were set to 2 fs and 50 ps, respectively. To examine the stability of ligand-binding mode, the root-mean-square displacement (RMSD) profiles of each system was computed over time, and crystal and docking complexes were compared.

Results and discussion

Predicted binding affinity corroborates experimental data

To get insights into the binding affinity of the phenolic compounds, binding energy (BE) scores were estimated (Table 1). All compounds were found to be HDAC binders as they showed a calculated BE ranging from − 5.31 to − 12.27 kcal/mol. Hence, they can all be said to be HDAC binders. It is interesting to note that curcumin showed a potential preference for HDAC8 while the rest of the compounds did not show potential selectivity neither for a specific HDAC isoform or a particular Class of HDAC.

Apigenin showed a lower BE score against HDAC8 (− 8.22 kcal/mol) compared with the rest of the study isoforms (> − 8.00 kcal/mol), while luteolin exhibited high binding propensity against HDACs 4, 6, 8, and 10 with respective BE values − 8.67, − 10.31, − 9.99, − 8.37 kcal/mol. Apigenin and luteolin displayed cancer cell growth inhibitory responses through the inhibition of class I HDACs (Pandey et al. 2012; Ganai et al. 2018). In another study, apigenin exhibited strong anticancer activity against non-small cell lung cancer cells through HDAC1 inhibition (Yan et al. 2020). Also, a recent computational study aiming at understanding the interaction between flavones and HDACs 1 and 2 showed that apigenin and luteolin bound to these HDACs well (Scafuri et al. 2020). Caffeic acid displayed strong binding to class I and IIb HDACs (BE ≤ − 9.00 kcal/mol). Caffeic acid and its derivatives have been known to have strong HDAC inhibitory activities (Bora-Tatar et al. 2009). The binding energy scores of chlorogenic acid are − 9.67, − 9.94, and − 11.50 kcal/mol for HDACs 4, 6, and 10. Chlorogenic acid has been shown to inhibit the growth of non-small cells through the inhibition of HDAC6 (Hongtao et al. 2018). Curcumin showed a potential preference for HDAC8,

Table 1 Binding energy (docking) scores of selected phenolic compounds against selected members of different classes of HDACs

Compound	Binding energy (kcal/mol)				
	Rep. Class I		Rep. Class IIa	Class IIb	
	HDAC1	HDAC8	HDAC4	HDAC6	HDAC10
Apigenin	− 7.68	− 8.22	− 7.83	− 7.24	− 7.15
Caffeic acid	− 9.03	− 9.06	− 7.98	− 9.62	− 9.36
Catechin	− 6.00	− 9.80	− 8.67	− 7.06	− 8.42
Chlorogenic acid	− 6.13	− 9.94	− 9.67	− 11.50	− 7.79
Curcumin	− 6.53	− 5.09	− 8.50	− 5.31	− 6.24
Gallic acid	− 7.60	− 9.46	− 8.71	− 9.91	− 9.59
Hyperoside	− 11.58	− 9.82	− 8.31	− 7.21	− 7.87
Kaempferol	− 7.68	− 9.43	− 9.34	− 7.13	− 8.57
Luteolin	− 6.89	− 9.99	− 8.67	− 10.31	− 8.37
Naringenin	− 7.61	− 8.20	− 7.59	− 8.08	− 8.52
p-hydroxybenzoic acid	− 7.22	− 8.23	− 7.48	− 8.99	− 8.82
Quercetin	− 6.14	− 10.77	− 9.33	− 10.60	− 9.09
Resveratrol	− 8.68	− 8.72	− 8.20	− 8.45	− 8.12
Rosmarinic acid	− 10.66	− 10.47	− 10.05	− 11.76	− 8.76
Rutin	− 9.66	− 12.27	− 12.05	− 8.34	− 9.99

Class I (1, 2, 3 and 8): representative members HDACs 1&8

Class IIa (4, 5, 7 and 9): representative member HDAC4

Class IIb (6 and 10): representative members HDACs 6 and 10

Class IV (11): no PDB structure, and no reliable template available for modeling

with affinity (BE = − 8.50 kcal/mol) compared to the other studied isoforms. The HDAC inhibitory activity of curcumin in various cancer cells including B-NHL cell Raji cell lines (Chen et al. 2007; Liu et al. 2005), medulloblastoma (Lee et al. 2011), and human lung cancer cell line (Namwan et al. 2022). Gallic acid demonstrated good binding propensity against all the study HDAC isoforms (HDAC1: − 7.60 kcal/mol, HDAC8: − 9.46 kcal/mol, HDAC4: − 8.71 kcal/mol, HDAC6: − 9.91 kcal/mol, and HDAC10: − 9.59 kcal/mol). Gallic acid slowed the progression of prostate cancer via inhibition of HDACs 1 and 2 (Jang et al. 2020). Interestingly, our docking study found that kaempferol possessed good inhibitory potential against all the study HDACs, with the strongest binding to HDAC8 (BE = − 9.43 kcal/mol). Consistently, in vitro profiling of zinc-containing human HDACs (classes I, II, and IV) revealed that kaempferol inhibited all the tested HDACs in human-derived hepatoma cell lines HepG2 and Hep3B; as well as HCT-116 colon cancer cells (Berger et al. 2013). Also, naringenin showed good binding potential against all the selected HDAC isoforms. Even though we have not found data on naringenin directly showing the activity of the compound on HDACs, its derivatives, 6- and 8-Prenylnaringenin demonstrated strong antitumor activity against melanoma through HDAC inhibition (Venturelli et al. 2018). It is also interesting to note that our molecular docking prediction, p-hydroxybenzoic acid displayed the highest binding propensity against HDAC6. In agreement with our data, p-hydroxybenzoic acid was shown to exhibit strong HDAC6 inhibition properties, modulating the microtubular structure and HSP90α chaperone activity in prostate cancer (Seidel et al. 2016). p-Hydroxybenzoic also showed HDAC6-specific inhibition which resulted in the enhancement of breast cancer sensitivity to Adriamycin (Wang et al. 2018). Polyphenol quercetin was reported to demonstrate in vitro HDAC8 inhibition and anticancer effects against colorectal cancer (Biswas et al. 2018). In agreement with the results from the study cited above, our docking calculations revealed quercetin to have the strongest binding to HDAC8 (BE = − 10.77 kcal/mol).

Furthermore, based on the BE cut-off values of ≤ − 8.00 kcal/mol, resveratrol, rutin and rosmarinic acid were found to demonstrate high inhibitory potential against all study HDAC isoforms, with rutin displaying the strongest binding. Resveratrol has been shown experimentally to have pan HDAC inhibitory activity on different solid tumors including hepatoblastoma (Gaetano et al. 2013), renal cell carcinoma (Dai et al. 2020), and prostate cancer (Dhar et al. 2015). Rutin, a natural flavonoid, inhibited HDAC6 activity and significantly increases α-tubulin acetylation level in motor neuron-like cells (Cetin et al. 2022). Rosmarinic acid induced cell cycle arrest and apoptosis via modulation of HDAC2 expression in prostate cancer (Jang et al. 2018). Note that even though our docking calculations showed that catechin, hyperoside bound to the study HDACs, to

the best of our knowledge, no experimental data suggesting their inhibitory activity against HDACs were found in the literature.

Catalytic mechanism of HDACs

Using HDAC8 enzyme, Lombardi et al. (2011) proposed that Zn^{2+} ion and the catalytically essential residue His143 promote the nucleophilic attack on zinc-bound water thereby making the nucleophilic lone electron pair available. The resulting oxyanion of the tetrahedral intermediate and its flanking transition states are stabilized by zinc coordination, as well as hydrogen bond interactions with Tyr306, His143, and two adjacent histidine residues His142, His143. These residues serve as a general acid catalyst in a "charge-relay" system to facilitate the collapse of the tetrahedral intermediate to form acetate and L-lysine on proton transfer, thought to be mediated by His143. The catalytic functions of His142 and His143 are influenced by H-bonding with Asp176 and Asp183, respectively (Lombardi et al. 2011).

Protein–ligand interaction

HDAC1-ligand interaction

Theπ crystal structure of HDAC1 in complex with a novel peptide inhibitor (PDB ID: 5ICN) revealed that the peptide ligand bound the enzyme with a typical cap-linker-chelator pharmacophore model. The cyclic part of the peptide occupied the wide entrance to the pocket, the extended region spanned the catalytic channel, and the C-terminal carboxyl group engaged the active site Zn^{2+} ion in metal-acceptor interaction. The peptide also interacted with catalytically essential residues His140, His141, Tyr303 via H-bonds. Other interactions formed include several van der Waals interactions and a couple of hydrophobic interactions (Fig. 1A).

Rutin formed several van der Waals interactions, including those with the catalytically essential amino acid residues His141, Tyr303; and H-bonds with Cys100, Ser148, and Gly149 via multiple hydroxyl groups. In addition, a couple of π-anion interactions with Asp99 and a π-π stacked interaction with Phe205 were formed. However, the Zn^{2+} ion was involved in van der Waals interaction (Fig. 1B). Similarly, rosmarinic acid engaged His141, Tyr303, Zn^{2+} ion and several active site residues in van der Waals interactions. It also formed H-bonds with Glu98, Asp99, and Gly149; π-π stacked interactions with Ph150 and Phe205 (Fig. 1C). The interaction between HDAC1 and other top compounds in terms of docking fitting scores for hyperoside, resveratrol, apigenin, and caffeic acid are similar to those described above (Figure S1). These interactions may be enough to inhibit the activity of the enzyme (Porter and Christianson 2019).

HDAC8-ligand interaction

The crystal ligand interacted with catalytically essential residues including the adjacent His142 and His143, and Tyr306 via H-bonds. However, the Zn^{2+} ion was engaged in van der Waals interaction (Fig. 2A). To validate our docking approach, the cocrystal ligand, hydroxamic acid-based inhibitor 4-naphthalen-1-yl-~(Uba and YelekÇİ)-oxidanyl-benzamide, was redocked into the active site of HDAC8. The RMSD between the cocrystal pose (grey) and docking poses was found to be 1.34 Å, indicating predictive ability of our docking method. The docking pose also interacted with His142 and Asp178 via H-bonds. However, the hydroxamic acid group interacted with His143 and Tyr306 via van der Waals interactions. Interestingly, the Zn^{2+} ion was engaged in metal-acceptor interaction (Fig. 2B). Also, both the crystal and docking poses formed π-π stacked interactions with Phe152, Phe208, and His180. In a similar manner, quercetin engaged the active site Zn^{2+} ion of HDAC8 via metal-acceptor interaction, and formed π-π stacked interactions with Phe152, Phe208, and His180. However, His142, His143, Tyr306 and more active site residues were engaged in van der Waals interaction with quercetin (Fig. 2C). Therefore, quercetin demonstrated similar binding mode to the linkerless hydroxamic acid-based inhibitor. Our previous computational study suggested that modifications around quercetin scaffold yielded potential HDAC inhibitors (Uba and YelekÇİ 2017). Other top compounds that interacted strongly with HDAC8 include rutin, rosmarinic acid, luteolin, and chlorogenic acid (Figure S2).

HDAC4-ligand interaction

The experimental binding mode of trifluoromethylketone inhibitor was visualized. The cocrystal ligand bound to HDAC4 through coordination with Zn^{2+} ion via diol group. The catalytic amino acid residues His158 and His159 are both engaged in H-bonds via hydroxyl from diol group. Also, His158, His159, Gly167, and Asp196 were involved in halogen interactions with trifluoryl substituent. Other interactions observed include π-sulfur interactions between the thiophene ring and Phe167 and His198, a π-π stacked interaction with Phe227, and a couple of van der Waals interactions all over the active site (Fig. 3A).

The docking pose was superimposed with the cocrystal pose with RMSD 1.35 Å even though the binding mode and orientation of the two ligand poses were almost the same (Fig. 3B). Like with the cocrystal pose, the docking pose formed a metal-acceptor interaction with Zn^{2+} ion via diol group, an H-bond with His158, halogen interactions with

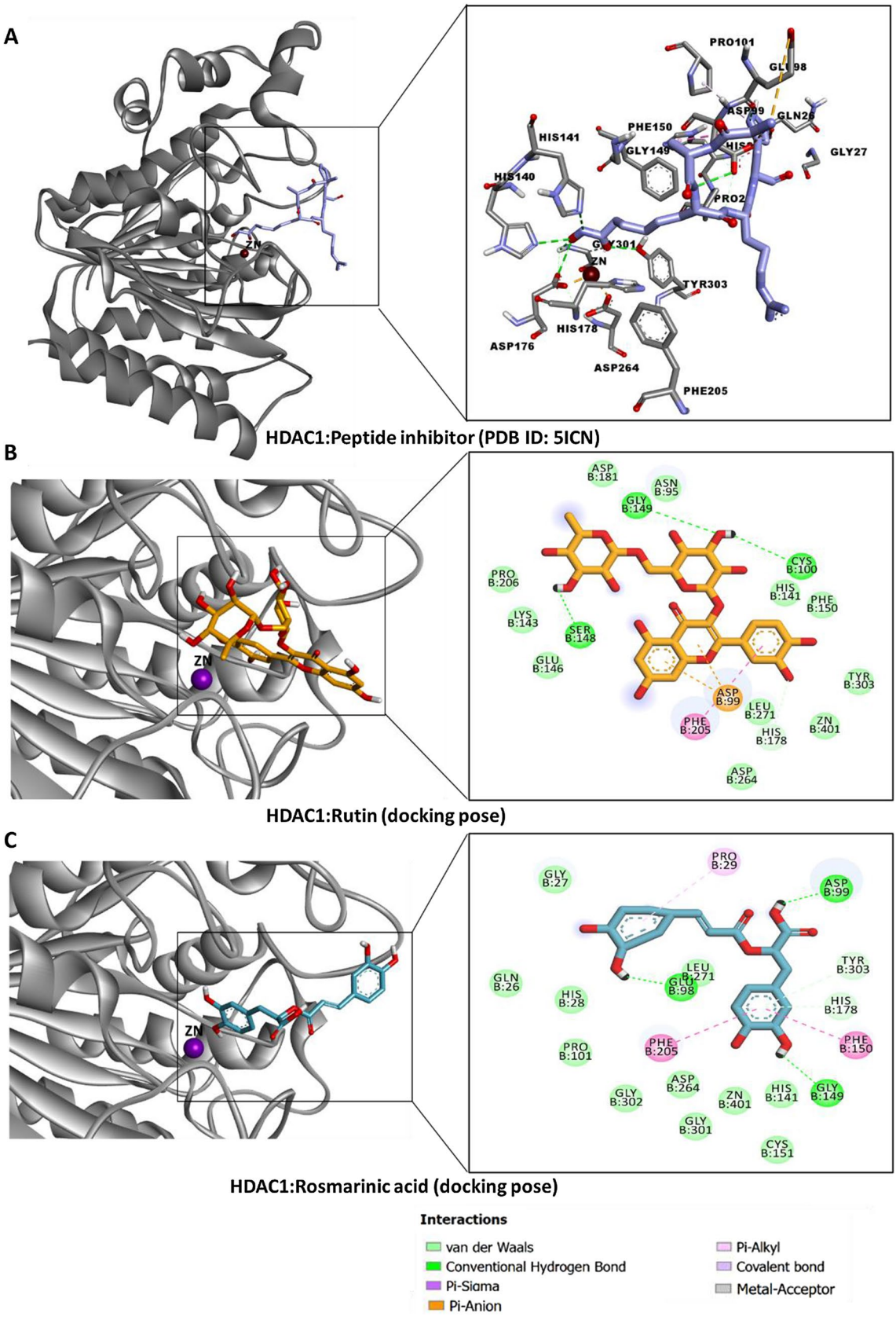

Fig. 1 **A** Crystal structure of HDAC1 complexed with a novel peptide inhibitor (PDB ID: 5ICN). **B** Docking poses and interaction of HDAC1 with rutin. **C** Docking pose and interaction of HDAC1 with rosmarinic acid

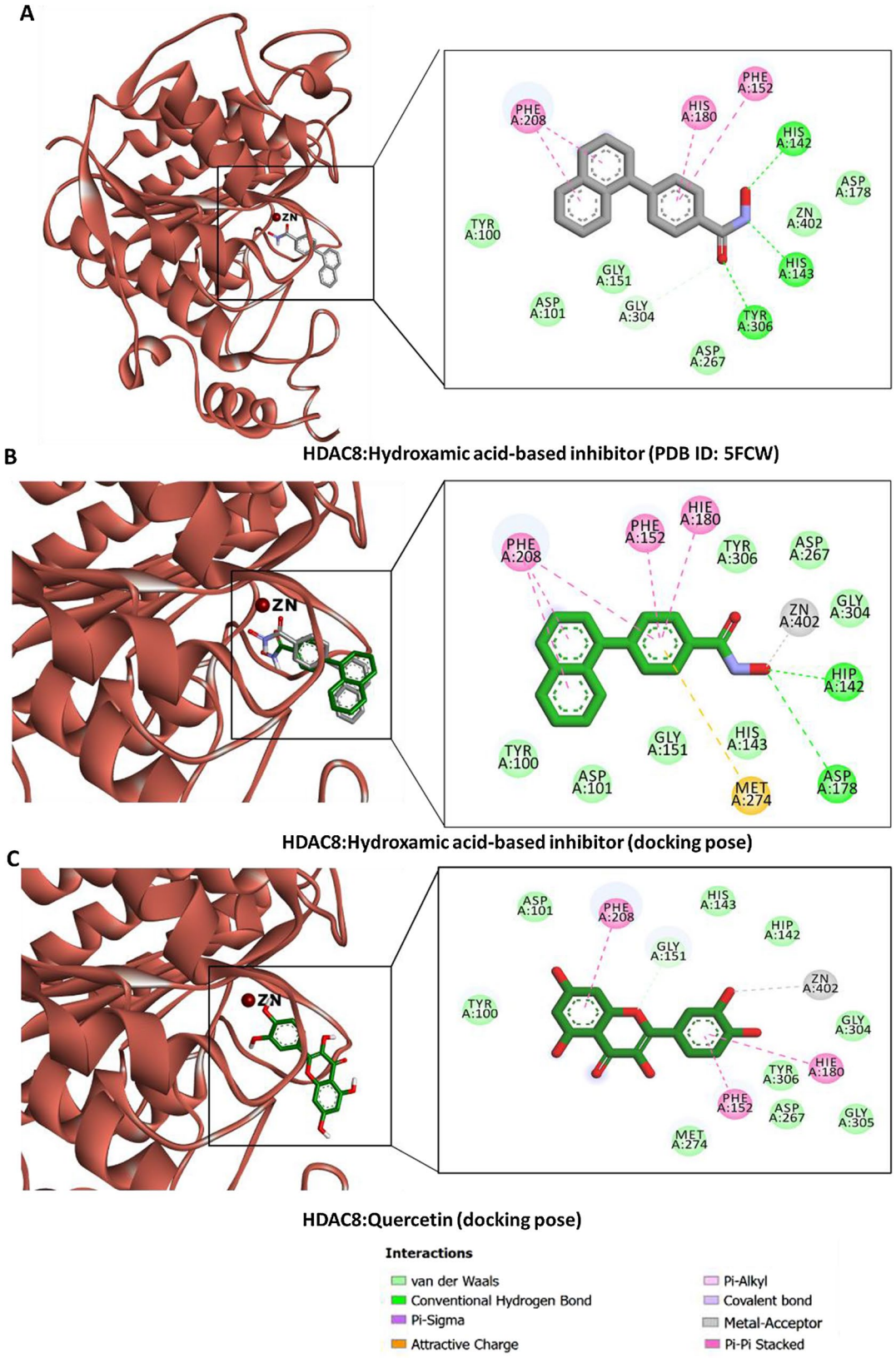

Fig. 2 Crystal structure of HDAC8 in complex with hydroxamic acid-based inhibitor (PDB ID: 5FCW). **A** Docking pose and interaction of hydroxamic acid-based inhibitor with HDAC8. **B** Docking pose and interaction of quercetin with HDAC8

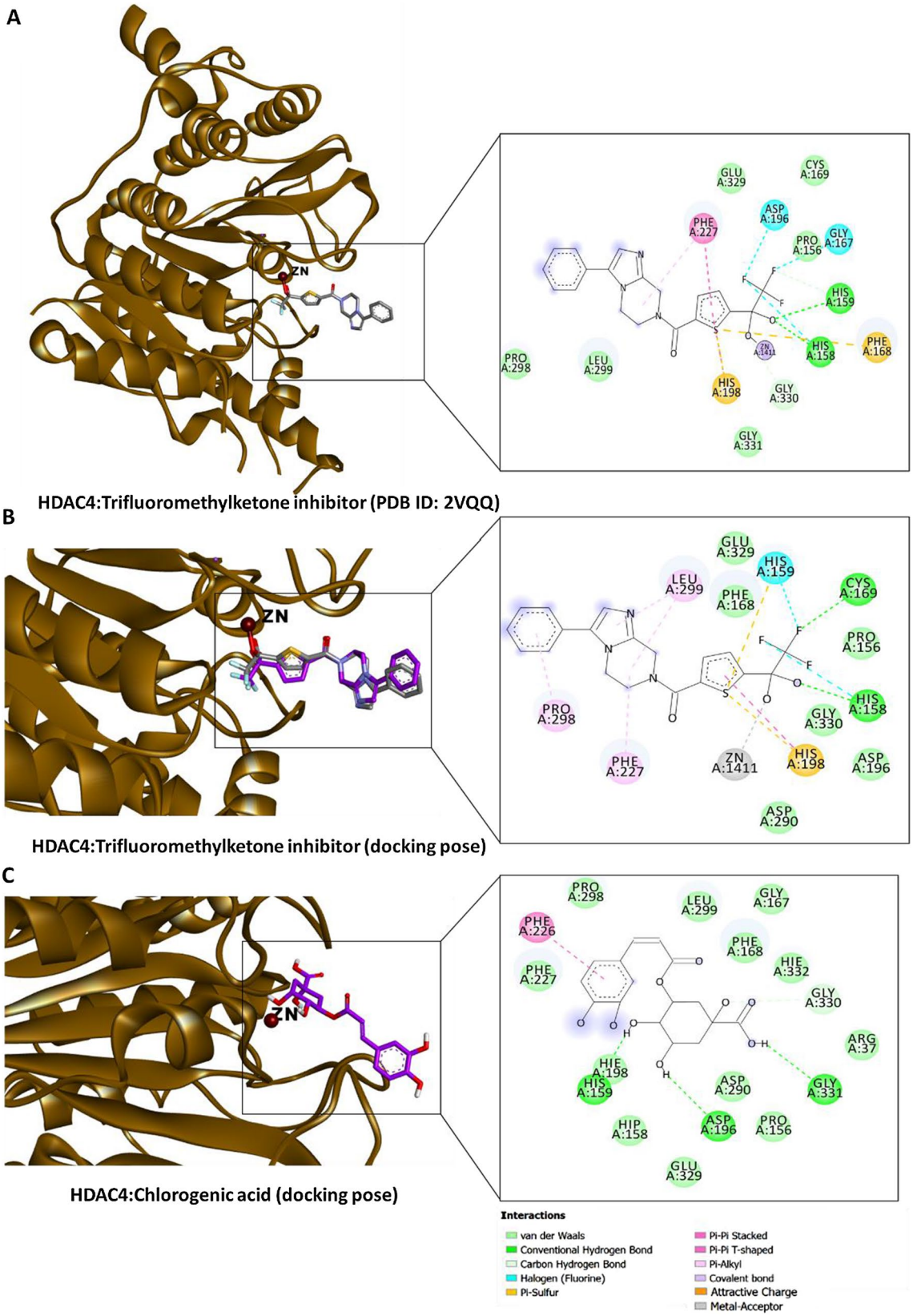

Fig. 3 **A** Crystal structure of HDAC4 in complex with trifluoromethylketone inhibitor (PDB ID: 2VQQ). **B** Docking pose and interaction of trifluoromethylketone inhibitor with HDAC4 (**C**) Docking pose and interaction of chlorogenic acid with HDAC4

His158 and His159 via trifluoryl substituent, and a π-sulfur interactions between the thiophene ring with His198. Other different interactions formed include a π-π stacked interaction between the thiophene ring of the ligand and His198, a couple of hydrophobic interactions near the entrance to the active site channel and few van der Waals interactions deep inside (Fig. 3B).

Chlorogenic acid occupied the active site of HDAC4 by forming different interactions including a H-bond with catalytic residue His158 and a van der Waals interaction with His159. Other interactions formed comprised H-bonds with Asp196 and Gly331 deep inside the catalytic channel, a π-π stacked interaction near the entrance to the pocket, and several van der Waals interactions all over the tunnel. Other compounds that demonstrated strong interactions with HDAC4 include rutin, kaempferol, rosmarinic acid, and quercetin (Figure S3). These interactions are likely to block the activity of the enzyme competitively (Tilekar et al. 2021) or allosterically by making it unavailable for interaction with other partners (Jayathilaka et al. 2012).

HDAC6-ligand interaction

The cocrystal ligand TSA, is a natural compound with potent inhibitory activity against class I and II HDACs (Sekhavat et al. 2007). TSA was bound to HDAC6 by forming strong coordination with Zn^{2+} ion via hydroxamic acid group. TSA also engaged a catalytic residue Tyr782 in H-bond interaction. Other interactions include van der Waals interaction with catalytic histidine residue His611 and several residues, π-sigma interactions with Phe620 and Phe680, and a hydrophobic interaction with Pro501 (Fig. 4A). The docking pose of TSA in HDAC6 active site is slightly different from the cocrystal pose, with RMSD of 1.92 Å. Similarly, in the docking pose, TSA engaged Zn^{2+} ion in metal-acceptor interaction via hydroxamic group, and formed an H-bond with catalytic His782, and a van der Waals interaction with His611. Other interactions include hydrophobic contacts with Phe620 and Pro501 and a few van der Waals interactions (Fig. 4B).

Although chlorogenic acid did not engage Zn^{2+} ion in any interaction, it formed van der Waals interactions with catalytic residues His610, His611, and Tyr782, as well as with other residues lining the active site. Other interactions include π-π stacked interactions with Phe620 and His651 deep inside the tunnel (Fig. 4C). Therefore, chlorogenic acid likely inhibits the activity of HDAC6 through these interactions since chlorogenic acid showed strong activity against non-small cell lung cancer through HDAC6 inhibition (Hongtao et al. 2018). Other compounds with strong binding to HDAC6 include rosmarinic acid, quercetin, luteolin, and gallic acid (Figure S4).

HDAC10-ligand interaction

The homology model of HDAC10 built using the crystal structure of *Danio rerio* (zebrafish) (PDB ID: 5TD7) was retrieved from our previous work (Ibrahim Uba and Yelekçi 2019). Docking analysis revealed that gallic acid and caffeic acid bound to HDAC10 in a similar mode. The two relatively smaller compounds, compared to classical HDAC inhibitors such as vorinostat, bound to HDAC10 such that their carbonyl group coordinated with Zn^{2+} ion via metal-acceptor interaction (Fig. 5). In addition, both gallic acid and caffeic acid were completely buried in the catalytic cavity of HDAC10, forming interaction with catalytically essential residues and the residue Glu272. Interestingly, rutin, p-hydroxybenzoic acid, quercetin, and rosmarinic acid also formed a H-bond with Glu272 (Figure S5). Glu272 is considered as a "gate keeper" residue responsible for potent HDAC10 binding (Géraldy et al. 2019).

Molecular dynamics simulation

MD simulations were carried out to evaluate the ligand-binding mode. Root-mean-square displacement (RMSD) was used a measure of structural stability, which is affected by ligand binding (Weako et al. 2020). The RMSD of the crystal structure of HDAC1 complexed with a novel peptide inhibitor (PDB ID: 5ICN) rose sharply to about 2.5 Å around 10 ns, and then converged between 2.0 and 2.6 Å until the end of the simulation. Similarly, the docking complex of HDAC1 with rutin reached an initial peak of about 2.0 Å quite earlier (around 4 ns), stabilized between 1.5 and 1.7 Å until around 35 ns, then increased and converged between 2.2 and 2.6 Å (Fig. 6A). While the crystal structure of HDAC8 in complex with hydroxamic acid-based inhibitor (PDB ID: 5FCW) reached RMSD convergence (between 1.3 and 1.7 Å) beyond 40 ns, the docking complex of HDAC8 with quercetin demonstrated a slightly higher RMSD trend, which beyond 42 ns, stabilized between 2.3 and 2.5 Å (Fig. 6B). The crystal structure of HDAC4 in complex with trifluoromethylketone inhibitor (PDB ID: 2VQQ) and the docking complex of HDAC4 with chlorogenic acid showed similar RMSD trends for the first 13 ns, the latter then slightly dropped and stabilized under 2.0 Å, while the former stabilized between 1.9 and 2.4 Å (Fig. 6C). Interestingly, the RMSDs of the crystal structure of HDAC6 in complex with trichostatin A (PDB ID: 5EDU) and the docking complex of HDAC6 with chlorogenic acid converged below 2.0 Å and synchronized beyond 10 ns until the end of the simulation

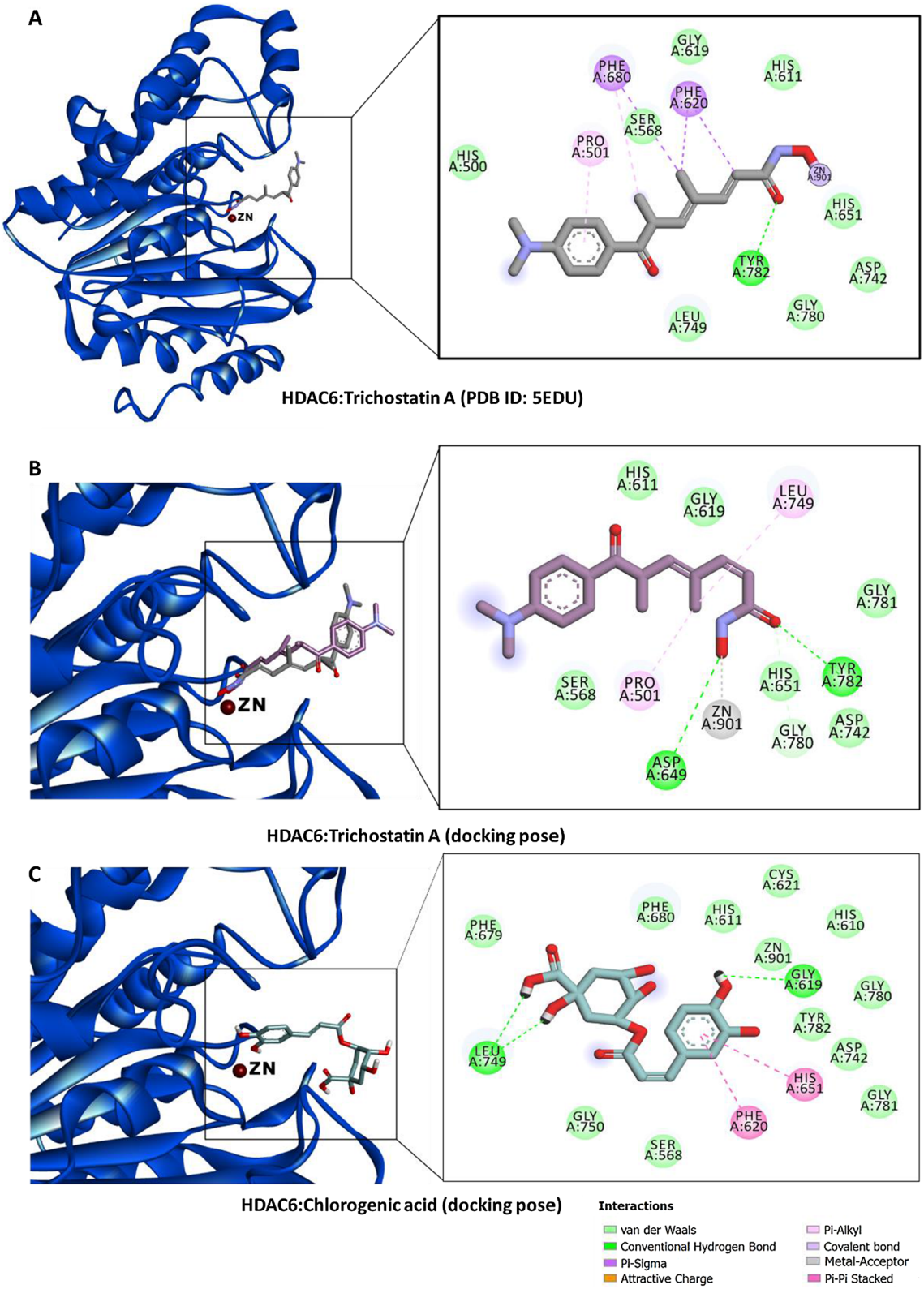

Fig. 4 **A** Crystal structure of HDAC6 in complex with trichostatin A (PDB ID: 5EDU). **B** Docking pose and interaction of trichostatin A with HDAC6. **C** Docking pose and interaction of quercetin with HDAC6

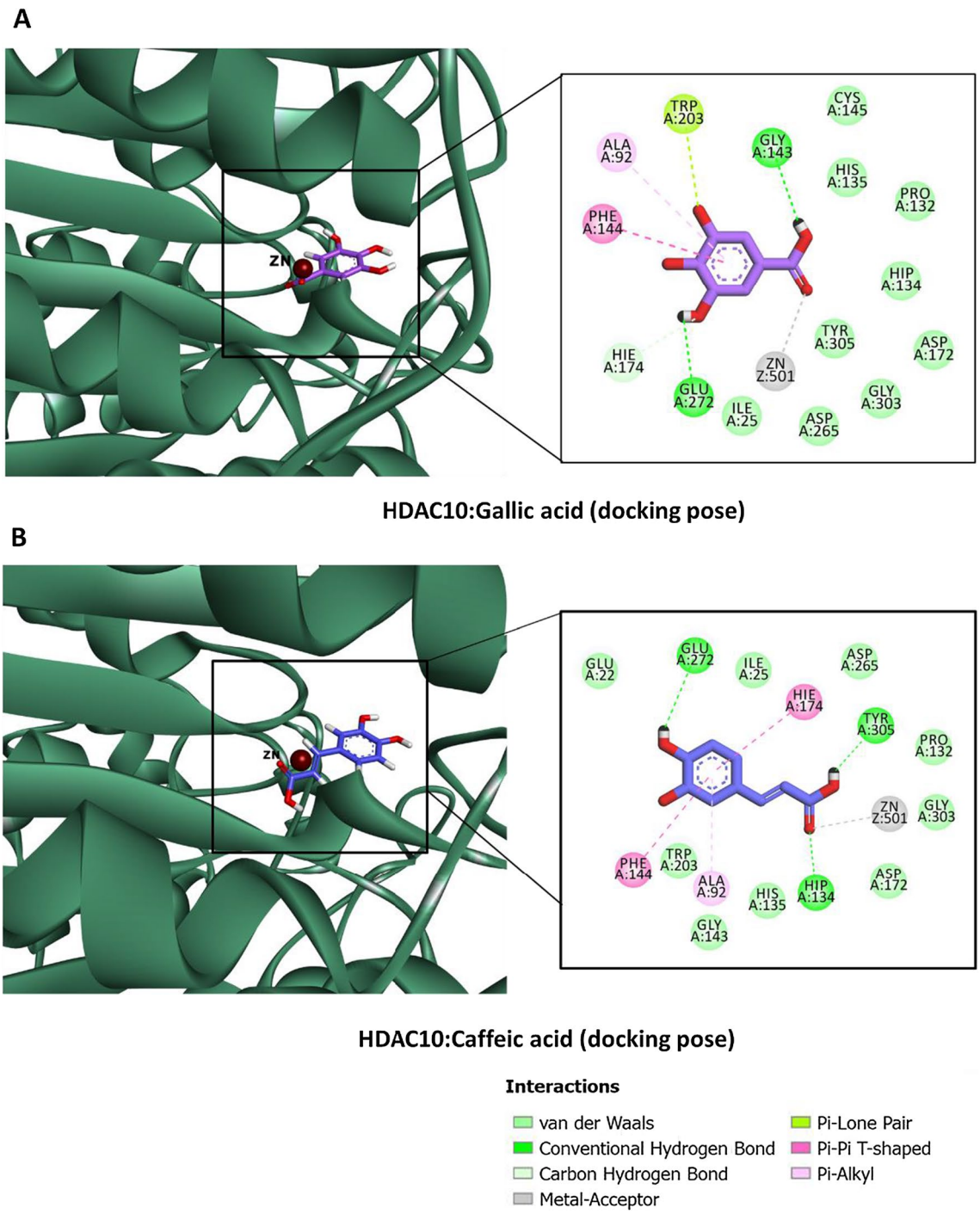

Fig. 5 **A** Docking pose and interaction of gallic acid with HDAC10 (human model) **B** Docking pose and interaction of caffeic acid with HDAC10 (human model)

(Fig. 6D). Finally, the unbound homology-modeled structure of HDAC10 and its docking complex with gallic acid showed higher but stable RMSD profiles (Fig. 6E). Similar trends were observed with the model and its complexes in our previous study (Ibrahim Uba and Yelekçi 2019; Uba and Yelekçi 2019).

Taken together, this study showed that phenolic compounds bind to different HDAC isoforms via interaction with catalytically essential residues with or without binding to the active site Zn^{2+} ion, corroborating with the results of several studies reporting the activity of these natural compounds against different HDACs. Furthermore, the some selected

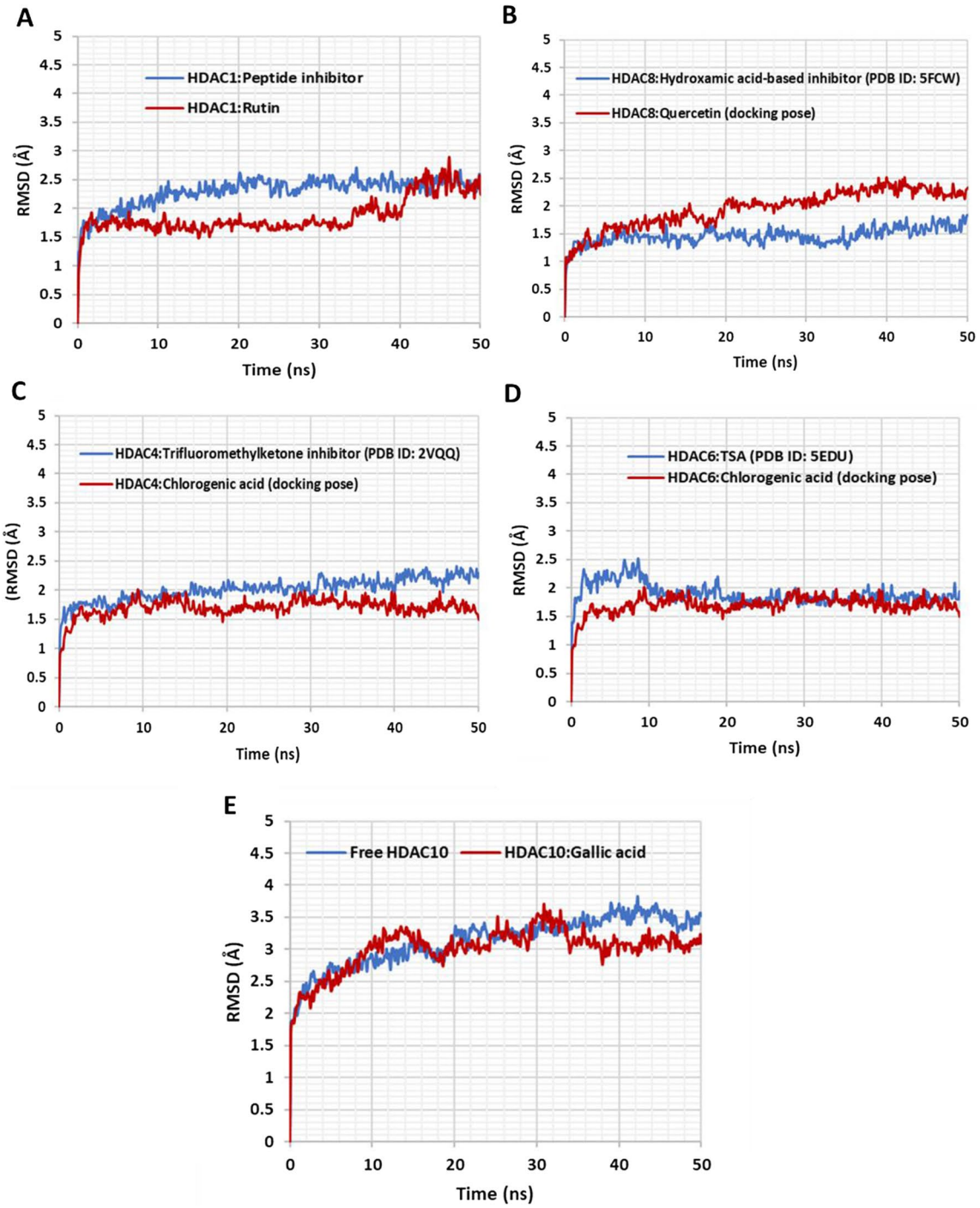

Fig. 6 Molecular dynamics simulation: root-mean square displacement (RMSD) profiles over 50 ns period. **A** Crystal structure of HDAC1 complexed with a novel peptide inhibitor (PDB ID: 5ICN) versus docking complex of HDAC1 with rutin. **B** Crystal structure of HDAC8 in complex with hydroxamic acid-based inhibitor (PDB ID: 5FCW) versus docking complex of HDAC8 with quercetin. **C** Crystal structure of HDAC4 in complex with trifluoromethylketone inhibitor (PDB ID: 2VQQ) versus docking complex of HDAC4 with chlorogenic acid. **D** Crystal structure of HDAC6 in complex with trichostatin A (PDB ID: 5EDU) versus docking complex of HDAC6 with chlorogenic acid. **E** Unbound homology-modeled structure of HDAC10 versus its docking complex with gallic acid

phenolic compounds showed a stable binding mode over 50 ns MD simulations.

Conclusion

Different phenolic compounds have been shown to possess

inhibitory activities against HDACs and are, therefore, considered safer alternatives to synthetic compounds. Here, we elucidated the binding mode and predicted the binding propensity of some of the top phenolic compounds against different isoforms representing different classes of HDACs using molecular docking approach. Our data reaffirmed the activity of the study phenolic compounds against HDACs. Also, binding interaction analysis suggests that these compounds can block the activity of HDACs with or without binding to the active site zinc metal ion. Furthermore, MD simulation examined binding mode stability of some selected phenolic compounds in the active site of the studied HDAC isoforms.

Supplementary Information The online version contains supplementary material available at https://doi.org/10.1007/s00726-023-03249-6.

Author contributions AIU and GZ carried out the study and wrote the manuscript. Both authors reviewed the manuscript.

Funding No funding.

Data availability The data used in this work are available upon request.

Declarations

Conflict of interest We declare that the authors have no competing interests.

References

Alseksek RK, Ramadan WS, Saleh E, El-Awady R (2022) The role of HDACs in the response of cancer cells to cellular stress and the potential for therapeutic intervention. Int J Mol Sci. https://doi.org/10.3390/ijms23158141

Berger A, Venturelli S, Kallnischkies M, Böcker A, Busch C, Weiland T, Noor S, Leischner C, Weiss TS, Lauer UM, Bischoff SC, Bitzer M (2013) Kaempferol, a new nutrition-derived pan-inhibitor of human histone deacetylases. J Nutr Biochem 24(6):977–985. https://doi.org/10.1016/j.jnutbio.2012.07.001

Biswas S, Reddy ND, Jayashree BS, Rao CM (2018) Evaluation of novel 3-hydroxyflavone analogues as HDAC inhibitors against colorectal cancer. Adv Pharmacol Sci 2018:1–14. https://doi.org/10.1155/2018/4751806

Bondarev AD, Attwood MM, Jonsson J, Chubarev VN, Tarasov VV, Schiöth HB (2021) Recent developments of HDAC inhibitors: emerging indications and novel molecules. Br J Clin Pharmacol 87(12):4577–4597. https://doi.org/10.1111/bcp.14889

Bora-Tatar G, Dayangaç-Erden D, Demir AS, Dalkara S, Yelekçi K, Erdem-Yurter H (2009) Molecular modifications on carboxylic acid derivatives as potent histone deacetylase inhibitors: activity and docking studies. Bioorg Med Chem 17(14):5219–5228. https://doi.org/10.1016/j.bmc.2009.05.042

Bornelöv S, Reynolds N, Xenophontos M, Gharbi S, Johnstone E, Floyd R, Ralser M, Signolet J, Loos R, Dietmann S, Bertone P, Hendrich B (2018) The nucleosome remodeling and deacetylation complex modulates chromatin structure at sites of active transcription to fine-tune gene expression. Mol Cell 71(1):56-72.e54. https://doi.org/10.1016/j.molcel.2018.06.003

Bottomley MJ, Lo Surdo P, Di Giovine P, Cirillo A, Scarpelli R, Ferrigno F, Jones P, Neddermann P, De Francesco R, Steinkühler C, Gallinari P, Carfí A (2008) Structural and functional analysis of the human HDAC4 catalytic domain reveals a regulatory structural zinc-binding domain. J Biol Chem 283(39):26694–26704. https://doi.org/10.1074/jbc.M803514200

Cetin O, Sari S, Erdem-Yurter H, Bora G (2022) Rutin increases alpha-tubulin acetylation via histone deacetylase 6 inhibition. Drug Dev Res 83(4):993–1002. https://doi.org/10.1002/ddr.21927

Chen Y, Shu W, Chen W, Wu Q, Liu H, Cui G (2007) Curcumin, both histone deacetylase and p300/CBP-specific inhibitor, represses the activity of nuclear factor kappa B and notch 1 in Raji cells. Basic Clin Pharmacol Toxicol 101(6):427–433. https://doi.org/10.1111/j.1742-7843.2007.00142.x

Dai L, Chen L, Wang W, Lin P (2020) Resveratrol inhibits ACHN cells via regulation of histone acetylation. Pharm Biol 58(1):231–238. https://doi.org/10.1080/13880209.2020.1738503

Dhar S, Kumar A, Li K, Tzivion G, Levenson AS (2015) Resveratrol regulates PTEN/Akt pathway through inhibition of MTA1/HDAC unit of the NuRD complex in prostate cancer. Biochim Biophys Acta 2:265–275. https://doi.org/10.1016/j.bbamcr.2014.11.004

Gaetano C, Venturelli S, Berger A, Böcker A, Busch C, Weiland T, Noor S, Leischner C, Schleicher S, Mayer M, Weiss TS, Bischoff SC, Lauer UM, Bitzer M (2013) Resveratrol as a pan-HDAC inhibitor alters the acetylation status of jistone proteins in human-derived hepatoblastoma cells. PLoS ONE. https://doi.org/10.1371/journal.pone.0073097

Ganai SA, Farooq Z, Banday S, Altaf M (2018) In silico approaches for investigating the binding propensity of apigenin and luteolin against class I HDAC isoforms. Future Med Chem 10(16):1925–1945. https://doi.org/10.4155/fmc-2018-0020

Gao L, Cueto MA, Asselbergs F, Atadja P (2002) Cloning and functional characterization of HDAC11, a novel member of the human histone deacetylase family. J Biol Chem 277(28):25748–25755. https://doi.org/10.1074/jbc.M111871200

Géraldy M, Morgen M, Sehr P, Steimbach RR, Moi D, Ridinger J, Oehme I, Witt O, Malz M, Nogueira MS, Koch O, Gunkel N, Miller AK (2019) Selective inhibition of histone deacetylase 10: hydrogen bonding to the gatekeeper residue is implicated. J Med Chem 62(9):4426–4443. https://doi.org/10.1021/acs.jmedchem.8b01936

Guenther MG, Barak O, Lazar MA (2001) The SMRT and N-CoR corepressors are activating cofactors for histone deacetylase 3. Mol Cell Biol 21(18):6091–6101. https://doi.org/10.1128/mcb.21.18.6091-6101.2001

Hai Y, Christianson DW (2016) Histone deacetylase 6 structure and molecular basis of catalysis and inhibition. Nat Chem Biol 12(9):741–747. https://doi.org/10.1038/nchembio.2134

Hai Y, Shinsky SA, Porter NJ, Christianson DW (2017) Histone deacetylase 10 structure and molecular function as a polyamine deacetylase. Nat Commun. https://doi.org/10.1038/ncomms15368

Hongtao L, Xiaoqi G, Junni L, Feng X, Guodong B, Liang Y (2018) Chlorogenic-induced inhibition of non-small cancer cells occurs through regulation of histone deacetylase 6. Cell Mol Biol (noisy-Le-Grand) 64(10):134–139. https://doi.org/10.14715/cmb/2018.64.10.22

Hu E, Chen Z, Fredrickson T, Zhu Y, Kirkpatrick R, Zhang G-F, Johanson K, Sung C-M, Liu R, Winkler J (2000) Cloning and characterization of a novel human class I Histone deacetylase that functions as a transcription repressor. J Biol Chem 275(20):15254–15264. https://doi.org/10.1074/jbc.M908988199

Hudson GM, Watson PJ, Fairall L, Jamieson AG, Schwabe JWR (2015) Insights into the recruitment of class IIa histone deacetylases (HDACs) to the SMRT/NCoR transcriptional repression complex.

J Biol Chem 290(29):18237–18244. https://doi.org/10.1074/jbc.M115.661058

Ibrahim Uba A, Yelekçi K (2019) Homology modeling of human histone deacetylase 10 and design of potential selective inhibitors. J Biomol Struct Dyn 37(14):3627–3636. https://doi.org/10.1080/07391102.2018.1521747

Jang YG, Hwang KA, Choi KC (2018) Rosmarinic acid, a component of rosemary tea, induced the cell cycle arrest and apoptosis through modulation of HDAC2 expression in prostate cancer cell lines. Nutrients. https://doi.org/10.3390/nu10111784

Jang Y-G, Ko E-B, Choi K-C (2020) Gallic acid, a phenolic acid, hinders the progression of prostate cancer by inhibition of histone deacetylase 1 and 2 expression. Journal Nutr Biochem. https://doi.org/10.1016/j.jnutbio.2020.108444

Jayathilaka N, Han A, Gaffney KJ, Dey R, Jarusiewicz JA, Noridomi K, Philips MA, Lei X, He J, Ye J, Gao T, Petasis NA, Chen L (2012) Inhibition of the function of class IIa HDACs by blocking their interaction with MEF2. Nucleic Acids Res 40(12):5378–5388. https://doi.org/10.1093/nar/gks189

Lee SJ, Krauthauser C, Maduskuie V, Fawcett PT, Olson JM, Rajasekaran SA (2011) Curcumin-induced HDAC inhibition and attenuation of medulloblastoma growth in vitro and in vivo. BMC Cancer. https://doi.org/10.1186/1471-2407-11-144

Lee J, Cheng X, Swails JM, Yeom MS, Eastman PK, Lemkul JA, Wei S, Buckner J, Jeong JC, Qi Y, Jo S, Pande VS, Case DA, Brooks CL, MacKerell AD, Klauda JB, Im W (2015) CHARMM-GUI input generator for NAMD, GROMACS, AMBER, OpenMM, and CHARMM/OpenMM simulations using the CHARMM36 additive force field. J Chem Theory Comput 12(1):405–413. https://doi.org/10.1021/acs.jctc.5b00935

Li Y, Seto E (2016) HDACs and HDAC inhibitors in cancer development and therapy. Cold Spring Harb Perspect Med. https://doi.org/10.1101/cshperspect.a026831

Li Y, Shin D, Kwon SH (2012) Histone deacetylase 6 plays a role as a distinct regulator of diverse cellular processes. FEBS J. https://doi.org/10.1111/febs.12079

Liu H-l, Chen Y, Cui G-h, Zhou J-f (2005) Curcumin, a potent antitumor reagent, is a novel histone deacetylase inhibitor regulating B-NHL cell line Raji proliferation. Acta Pharmacol Sin 26(5):603–609. https://doi.org/10.1111/j.1745-7254.2005.00081.x

Lombardi PM, Angell HD, Whittington DA, Flynn EF, Rajashankar KR, Christianson DW (2011) Structure of prokaryotic polyamine deacetylase reveals evolutionary functional relationships with eukaryotic histone deacetylases. Biochemistry 50(11):1808–1817. https://doi.org/10.1021/bi101859k

Losson H, Schnekenburger M, Dicato M, Diederich M (2016) Natural compound histone deacetylase inhibitors (HDACi): synergy with inflammatory signaling pathway modulators and clinical applications in cancer. Molecules. https://doi.org/10.3390/molecules21111608

Martínez-Rosell G, Giorgino T, De Fabritiis G (2017) PlayMolecule proteinprepare: a web application for protein preparation for molecular dynamics simulations. J Chem Inf Model 57(7):1511–1516. https://doi.org/10.1021/acs.jcim.7b00190

Milazzo G, Mercatelli D, Di Muzio G, Triboli L, De Rosa P, Perini G, Giorgi FM (2020) Histone deacetylases (HDACs): evolution, specificity, role in transcriptional complexes, and pharmacological actionability. Genes. https://doi.org/10.3390/genes11050556

Miteva MA, Guyon F, Tuffery P (2010) Frog2: Efficient 3D conformation ensemble generator for small compounds. Nucleic Acids Res 38(Web Server):W622–W627. https://doi.org/10.1093/nar/gkq325

Moreno-Yruela C, Galleano I, Madsen AS, Olsen CA (2018) Histone deacetylase 11 Is an ε-N-myristoyllysine hydrolase. Cell Chem Biol 25(7):849-856.e848. https://doi.org/10.1016/j.chembiol.2018.04.007

Morris GM, Huey R, Lindstrom W, Sanner MF, Belew RK, Goodsell DS, Olson AJ (2009) AutoDock4 and AutoDockTools4: Automated docking with selective receptor flexibility. J Comput Chem 30(16):2785–2791. https://doi.org/10.1002/jcc.21256

Muslin A (2000) 14–3-3 proteins: regulation of subcellular localization by molecular interference. Cell Signal 12(11–12):703–709. https://doi.org/10.1016/s0898-6568(00)00131-5

Namwan N, Senawong G, Phaosiri C, Kumboonma P, Somsakeesit L-o, Samankul A, Leerat C, Senawong T (2022) HDAC inhibitory and anti-cancer activities of curcumin and curcumin derivative CU17 against human lung cancer A549 cells. Molecules. https://doi.org/10.3390/molecules27134014

Panda V, Laddha A, Nandave M, Srinath S (2016) Dietary phenolic acids ofmacrotyloma uniflorum(Horse Gram) protect the rat heart against isoproterenol-induced myocardial infarction. Phytother Res 30(7):1146–1155. https://doi.org/10.1002/ptr.5620

Pandey M, Kaur P, Shukla S, Abbas A, Fu P, Gupta S (2012) Plant flavone apigenin inhibits HDAC and remodels chromatin to induce growth arrest and apoptosis in human prostate cancer cells: in vitro and in vivo study. Mol Carcinog 51(12):952–962. https://doi.org/10.1002/mc.20866

Pant K, Peixoto E, Richard S, Gradilone SA (2020) Role of histone deacetylases in carcinogenesis: potential role in cholangiocarcinoma. Cells. https://doi.org/10.3390/cells9030780

Park S-Y, Kim J-S (2020) A short guide to histone deacetylases including recent progress on class II enzymes. Exp Mol Med 52(2):204–212. https://doi.org/10.1038/s12276-020-0382-4

Phillips JC, Braun R, Wang W, Gumbart J, Tajkhorshid E, Villa E, Chipot C, Skeel RD, Kale L, Schulten K (2005) Scalable molecular dynamics with NAMD. J Comput Chem 26(16):1781–1802. https://doi.org/10.1002/jcc.20289

Porter NJ, Christianson DW (2019) Structure, mechanism, and inhibition of the zinc-dependent histone deacetylases. Curr Opin Struct Biol 59:9–18. https://doi.org/10.1016/j.sbi.2019.01.004

Roy AJ, Stanely Mainzen Prince P (2013) Preventive effects of p-coumaric acid on cardiac hypertrophy and alterations in electrocardiogram, lipids, and lipoproteins in experimentally induced myocardial infarcted rats. Food Chem Toxicol 60:348–354. https://doi.org/10.1016/j.fct.2013.04.052

Saunders A, Huang X, Fidalgo M, Reimer MH, Faiola F, Ding J, Sánchez-Priego C, Guallar D, Sáenz C, Li D, Wang J (2017) The SIN3A/HDAC corepressor complex functionally cooperates with NANOG to promote pluripotency. Cell Rep 18(7):1713–1726. https://doi.org/10.1016/j.celrep.2017.01.055

Scafuri B, Bontempo P, Altucci L, De Masi L, Facchiano A (2020) Molecular docking simulations on histone deacetylases (HDAC)-1 and -2 to investigate the flavone binding. Biomedicines. https://doi.org/10.3390/biomedicines8120568

Seidel C, Schnekenburger M, Mazumder A, Teiten M-H, Kirsch G, Dicato M, Diederich M (2016) 4-Hydroxybenzoic acid derivatives as HDAC6-specific inhibitors modulating microtubular structure and HSP90α chaperone activity against prostate cancer. Biochem Pharmacol 99:31–52. https://doi.org/10.1016/j.bcp.2015.11.005

Sekhavat A, Sun J-M, Davie JR (2007) Competitive inhibition of histone deacetylase activity by trichostatin A and butyrate. Biochem Cell Biol 85(6):751–758. https://doi.org/10.1139/o07-145

Shimizu K, Mira A (2015) In vitro cytotoxic activities and molecular mechanisms of angelica shikokiana extract and its isolated compounds. Pharmacogn Mag. https://doi.org/10.4103/0973-1296.172962

Shukla S, Tekwani BL (2020) Histone deacetylases inhibitors in neurodegenerative, diseases neuroprotection and neuronal

differentiation. Front Pharmacol. https://doi.org/10.3389/fphar.2020.00537

Simões-Pires C, Zwick V, Nurisso A, Schenker E, Carrupt P-A, Cuendet M (2013) HDAC6 as a target for neurodegenerative diseases: what makes it different from the other HDACs? Mol Neurodegener. https://doi.org/10.1186/1750-1326-8-7

Tabackman AA, Frankson R, Marsan ES, Perry K, Cole KE (2016) Structure of 'linkerless' hydroxamic acid inhibitor-HDAC8 complex confirms the formation of an isoform-specific subpocket. J Struct Biol 195(3):373–378. https://doi.org/10.1016/j.jsb.2016.06.023

Tilekar K, Hess JD, Upadhyay N, Schweipert M, Flath F, Gutierrez DA, Loiodice F, Lavecchia A, Meyer-Almes FJ, Aguilera RJ, Ramaa CS (2021) HDAC4 inhibitors with cyclic linker and non-hydroxamate zinc binding group: design, synthesis, HDAC screening and in vitro cytotoxicity evaluation. Chem Select 6(26):6748–6763. https://doi.org/10.1002/slct.202102061

Tsuji N, Kobayashi M, Nagashima K, Wakisaka Y, Koizumi K (1976) A new antifungal antibiotic, trichostatin. J Antibiot 29(1):1–6. https://doi.org/10.7164/antibiotics.29.1

Uba AI, Yelekçi K (2017) Identification of potential isoform-selective histone deacetylase inhibitors for cancer therapy: a combined approach of structure-based virtual screening, ADMET prediction and molecular dynamics simulation assay. J Biomol Struct Dyn 36(12):3231–3245. https://doi.org/10.1080/07391102.2017.1384402

Uba Aİ, YelekÇİ K (2017) Exploration of the binding pocket of histone deacetylases: the design of potent and isoform-selective inhibitors. Turk J Biol 41:901–918. https://doi.org/10.3906/biy-1701-26

Uba AI, Yelekçi K (2018a) Carboxylic acid derivatives display potential selectivity for human histone deacetylase 6: structure-based virtual screening, molecular docking and dynamics simulation studies. Comput Biol Chem 75:131–142. https://doi.org/10.1016/j.compbiolchem.2018.05.004

Uba AI, Yelekçi K (2018b) Pharmacophore-based virtual screening for identification of potential selective inhibitors of human histone deacetylase 6. Comput Biol Chem 77:318–330. https://doi.org/10.1016/j.compbiolchem.2018.10.016

Uba AI, Yelekçi K (2019) Crystallographic structure versus homology model: a case study of molecular dynamics simulation of human and zebrafish histone deacetylase 10. J Biomol Struct Dyn 38(15):4397–4406. https://doi.org/10.1080/07391102.2019.1691658

Venturelli S, Niessner H, Sinnberg T, Berger A, Burkard M, Urmann C, Donaubauer K, Böcker A, Leischner C, Riepl H, Frank J, Lauer Ulrich M, Garbe C, Busch C (2018) 6- and 8-prenylnaringenin, novel natural histone deacetylase inhibitors found in hops, exert antitumor activity on melanoma cells. Cell Physiol Biochem 51(2):543–556. https://doi.org/10.1159/000495275

Volmar C-H, Wahlestedt C (2015) Histone deacetylases (HDACs) and brain function. Neuroepigenetics 1:20–27. https://doi.org/10.1016/j.nepig.2014.10.002

Wang F, Lu W, Zhang T, Dong J, Gao H, Li P, Wang S, Zhang J (2013) Development of novel ferulic acid derivatives as potent histone deacetylase inhibitors. Bioorg Med Chem 21(22):6973–6980. https://doi.org/10.1016/j.bmc.2013.09.021

Wang XN, Wang KY, Zhang XS, Yang C, Li XY (2018) 4-Hydroxybenzoic acid (4-HBA) enhances the sensitivity of human breast cancer cells to adriamycin as a specific HDAC6 inhibitor by promoting HIPK2/p53 pathway. Biochem Biophys Res Commun 504(4):812–819. https://doi.org/10.1016/j.bbrc.2018.08.043

Wang P, Wang Z, Liu J (2020) Role of HDACs in normal and malignant hematopoiesis. Mol Cancer. https://doi.org/10.1186/s12943-019-1127-7

Watson PJ, Fairall L, Santos GM, Schwabe JWR (2012) Structure of HDAC3 bound to co-repressor and inositol tetraphosphate. Nature 481(7381):335–340. https://doi.org/10.1038/nature10728

Watson PJ, Millard CJ, Riley AM, Robertson NS, Wright LC, Godage HY, Cowley SM, Jamieson AG, Potter BVL, Schwabe JWR (2016) Insights into the activation mechanism of class I HDAC complexes by inositol phosphates. Nat Commun. https://doi.org/10.1038/ncomms11262

Weako J, Uba AI, Keskin Ö, Gürsoy A, Yelekçi K (2020) Identification of potential inhibitors of human methionine aminopeptidase (type II) for cancer therapy: structure-based virtual screening, ADMET prediction and molecular dynamics studies. Comput Biol Chem. https://doi.org/10.1016/j.compbiolchem.2020.107244

Yan W, Wu THY, Leung SSY, To KKW (2020) Flavonoids potentiated anticancer activity of cisplatin in non-small cell lung cancer cells in vitro by inhibiting histone deacetylases. Life Sci. https://doi.org/10.1016/j.lfs.2020.118211

You A, Tong JK, Grozinger CM, Schreiber SL (2001) CoREST is an integral component of the CoREST- human histone deacetylase complex. Proc Natl Acad Sci 98(4):1454–1458. https://doi.org/10.1073/pnas.98.4.1454

Zhang Y, Gilquin B, Khochbin S, Matthias P (2006) Two catalytic domains are required for protein deacetylation. J Biol Chem 281(5):2401–2404. https://doi.org/10.1074/jbc.C500241200